Supplementary Information for

"Backside illumination-enabled metrology and inspection inside 3D-ICs using frequency comb-based chromatic confocal and spectral interferometry"

Hyoungsu Choi,¹ Hyunsoo Kwak,² Sungyoon Ryu,² Younghoon Sohn,² and Jungwon Kim¹,*

¹ Korea Advanced Institute of Science and Technology (KAIST), Daejeon 34141, Korea

² Samsung Electronics Co. Ltd., Gyeonggi-do 18448, Korea

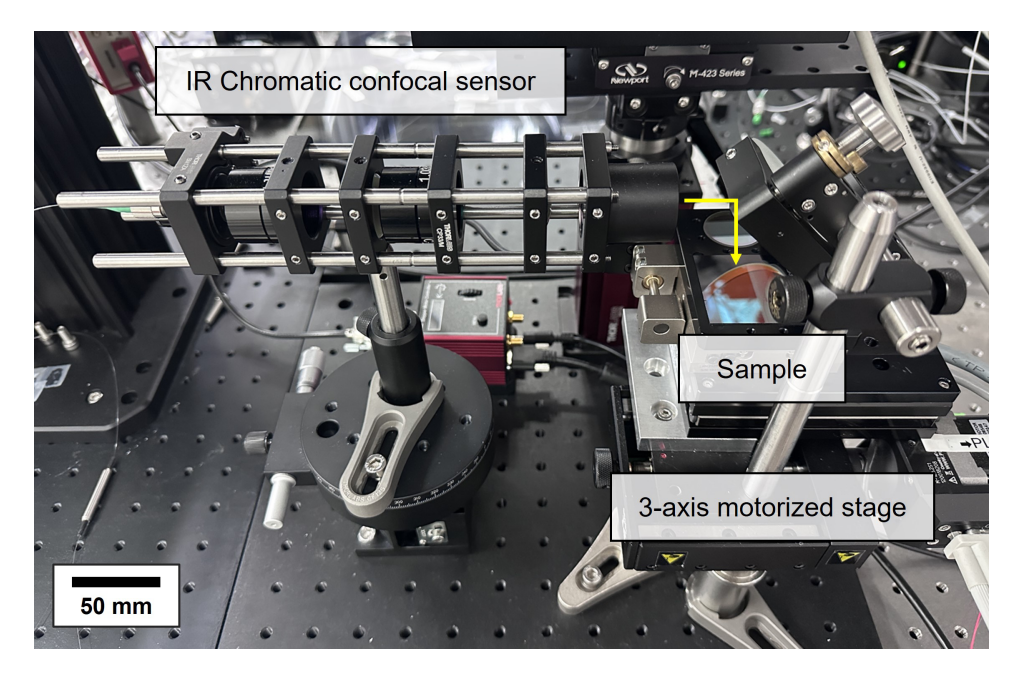


Figure S1 | **Experimental setup with IR chromatic confocal optical sensor.** The optical frequency comb is coupled into the IR chromatic confocal sensor, which focuses the beam onto the sample mounted on the 3-axis motorized stage.

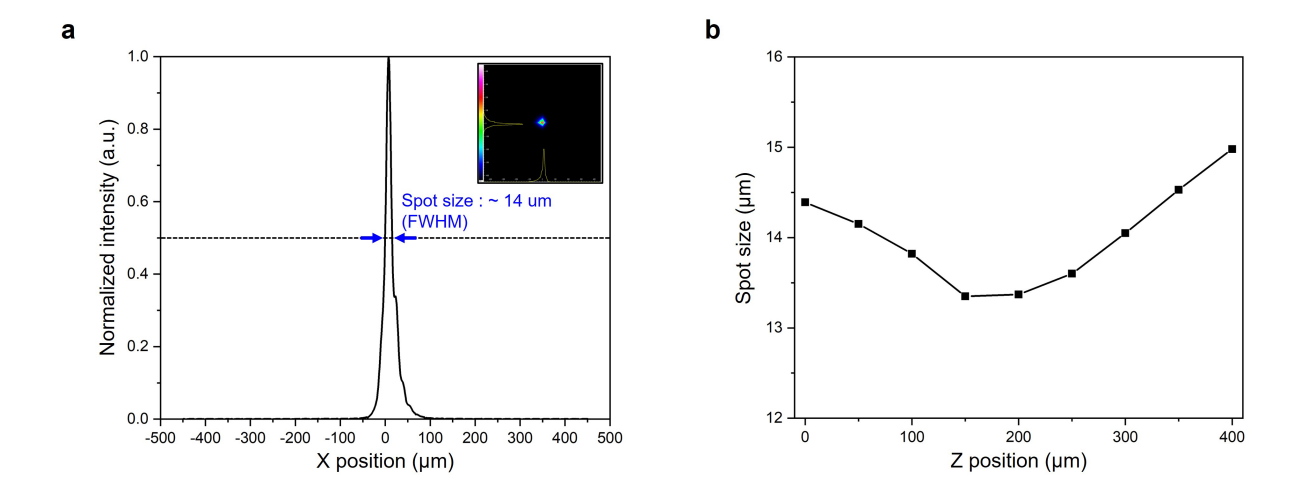


Figure S2 | **Spot size performance of the IR chromatic confocal sensor. a**, Spot size of the IR chromatic confocal sensor measured using a beam profiler. **b**, Variation of the spot size along the Z-axis.

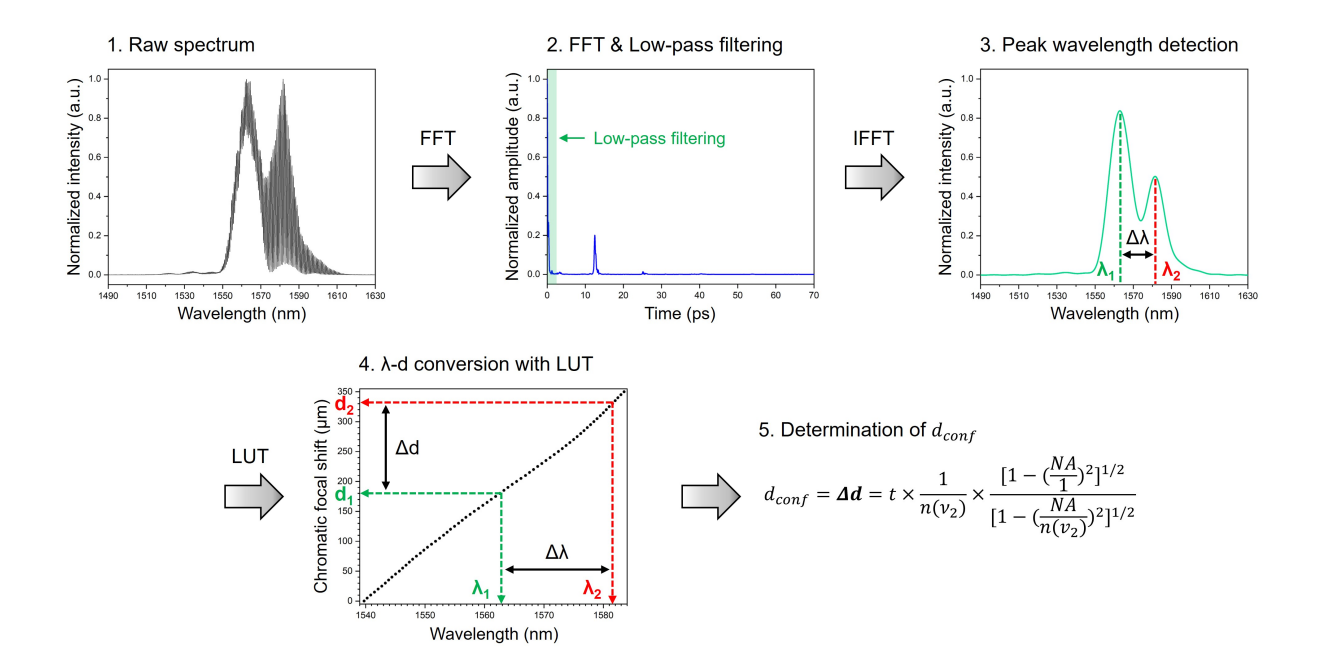


Figure S3 | Chromatic confocal signal analysis in the chromatic confocal spectral interferometry method.

The spectrum acquired by the optical spectrum analyzer (OSA) is first k-linearized and then Fourier-transformed. A low-pass filter is applied, and the filtered signal is inverse Fourier transformed to obtain the two spectral peaks corresponding to the center wavelengths λ_1 and λ_2 . A look-up table (LUT) is constructed from a calibration spectrum measured from a mirror using the same filtering process. This LUT enables the conversion of the measured spectral shift $\Delta\lambda$ into a depth difference Δd , from which the chromatic confocal thickness d_{conf} is calculated.

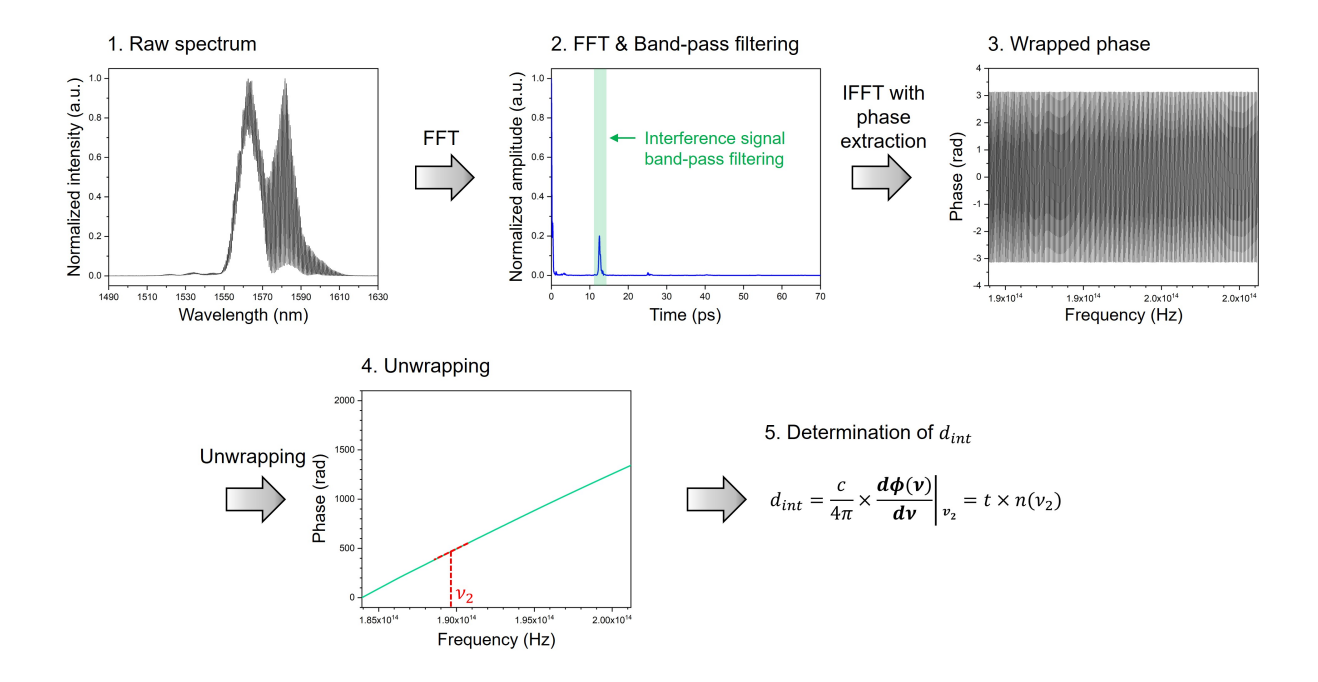


Figure S4 | Interference signal analysis in the chromatic confocal spectral interferometry method. The spectrum acquired by the OSA is first k-linearized and then Fourier-transformed. A band-pass filter is applied to isolate the primary interference signal by removing unwanted multi-reflection components within the silicon wafer. The filtered signal is then inverse Fourier transformed, resulting in a complex-valued signal that retains intensity information. To extract the phase component, the natural logarithm is applied to the IFFT result, from which the imaginary part corresponding to the phase is retrieved. The obtained wrapped phase is unwrapped, and the slope at the center frequency v_2 , corresponding to the center wavelength λ_2 , is calculated. This slope is subsequently used to determine the interferometric optical thickness d_{int} .

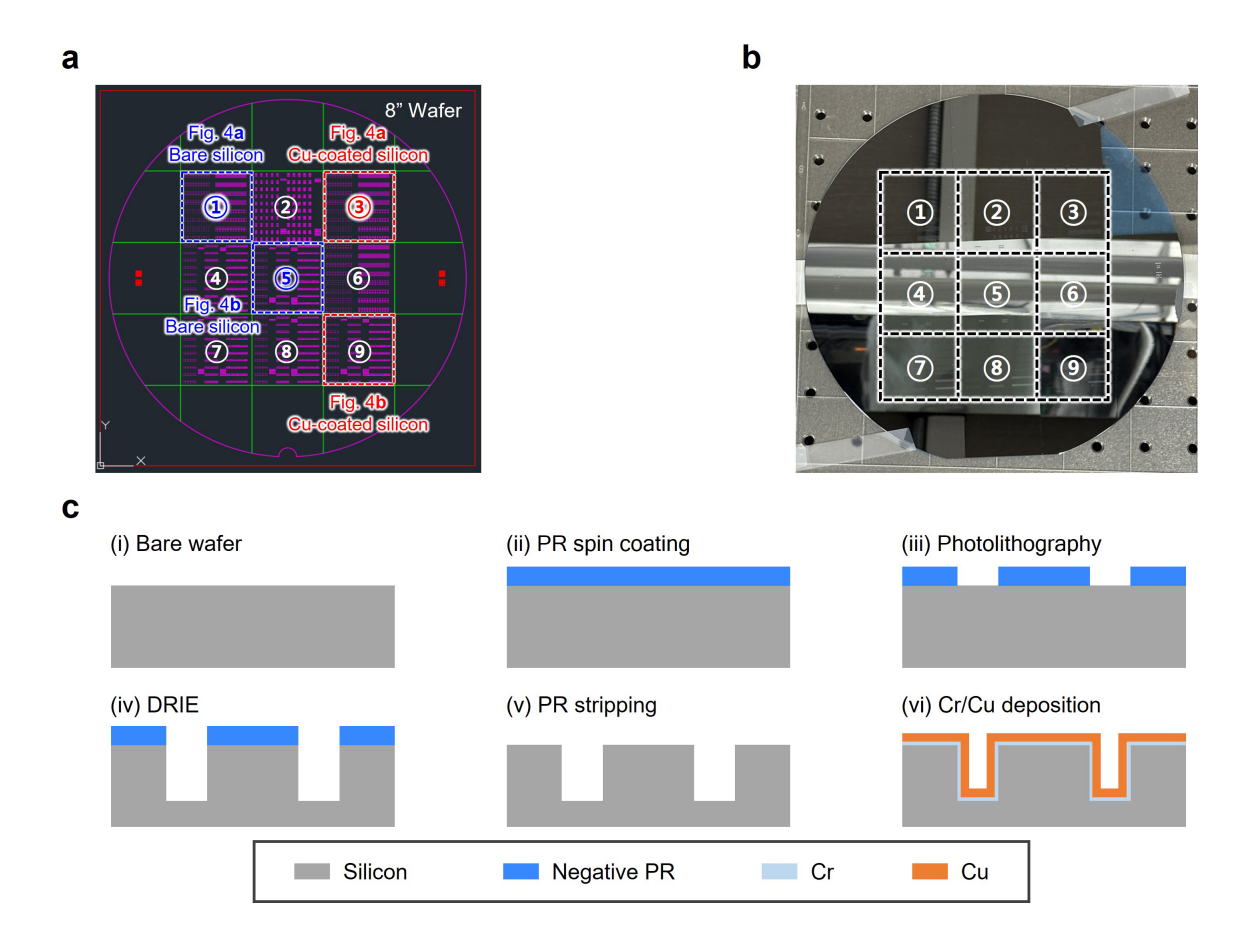


Figure S5 | **Silicon sample fabrication process and results. a**, Photolithography mask design for an 8-inch wafer, divided into nine dies, and used for the demonstration in Fig. 4. **b**, Photograph of the fabricated silicon wafer with patterned regions corresponding to the mask layout. **c**, Fabrication process flow: (i) bare silicon wafer, (ii) negative photoresist (PR) spin coating, (iii) photolithography, (iv) deep reactive ion etching (DRIE), (v) PR stripping, (vi) Cr/Cu deposition.

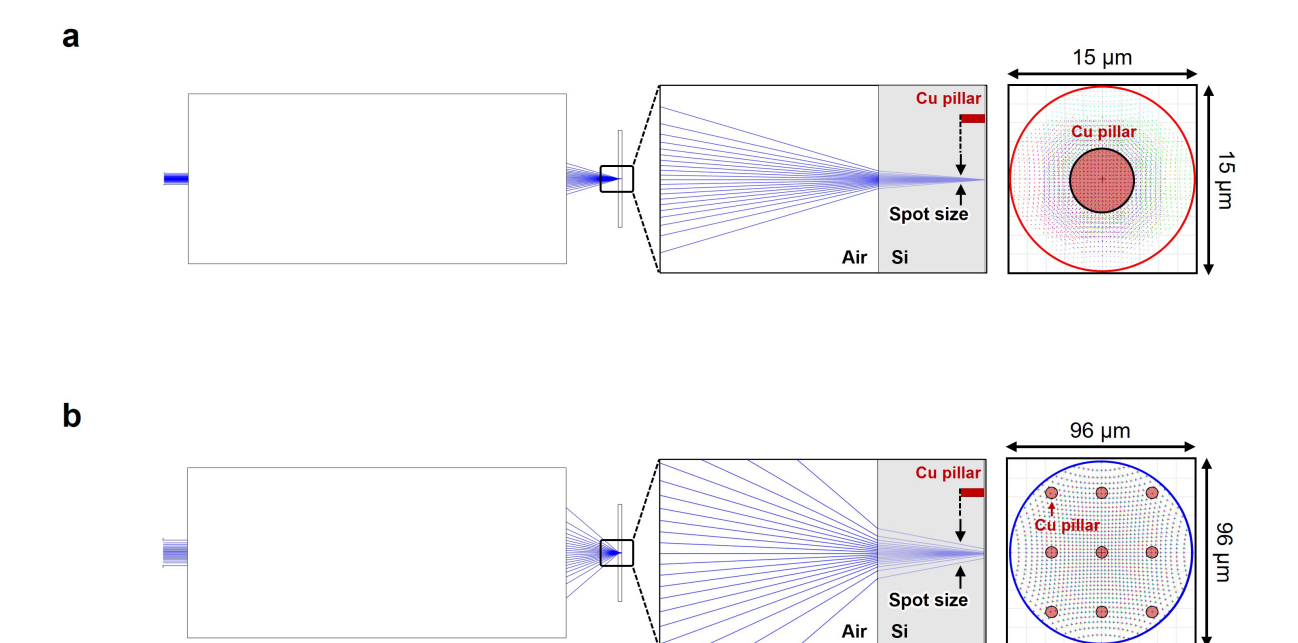


Figure S6 | **Optical simulation results for the TSV measurement setup a**, Optical simulation of the measurement setup for a single Cu-filled TSV. **b**, Optical simulation of the measurement setup for a Cu-filled TSV array.

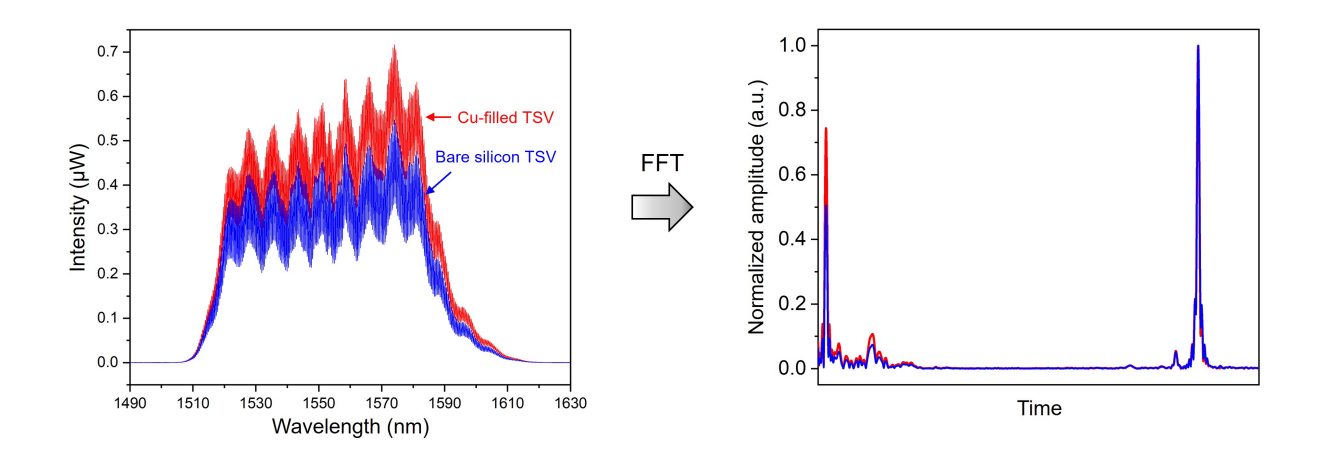


Figure S7 | Comparison of reflection spectra from Cu-filled and bare silicon holes. The left panel presents the reflection spectra acquired from a Cu-filled TSV (red) and a bare silicon TSV (blue). The right panel shows the corresponding time-domain signals obtained via Fourier transform, where both Cu-filled and bare silicon TSVs exhibit identical peak positions.

Source of uncertainty errors	Value	Value (nm) for L_0 =232 mm L_1 =725.4 μm and n=3.512
① Systematic uncertainty of the interferometry	$\sqrt{(2)^2 + (3)^2 + (4)^2}$	479.8
② Uncertainty of DFT algorithm $(L_1 \cdot n)$	479.5 nm	
③ Uncertainty of OSA (0.01 nm)	$6.6\times 10^{-6}\cdot L_1\cdot n$	
4 Uncertainty related to refractive index of air	$3.0\times 10^{-8}\cdot L_0$	
(5) Statistical uncertainty analysis of the interferometry	$\sqrt{6}^2$	55.8
Measurement repeatability of the interferometry	55.8 nm	
a Combined uncertainty of the interferometry	(a) $=\sqrt{(1)^2+(5)^2}$	483.0
Systematic uncertainty of the chromatic confocal	$\sqrt{8^2 + 9^2 + 10^2 + 11^2}$	298.3
(8) Uncertainty of LUT (OSA: 0.04nm/step)	296 nm	
Uncertainty of motor stage movement	$2.0\cdot 10^{-5}\cdot \frac{L_1}{n}$	
(10) Uncertainty of calibration mirror flatness	36 nm	
① Uncertainty of refractive index of air	$3.0\times 10^{-8}\cdot L_0$	
② Statistical uncertainty analysis of the chromatic confocal	$\sqrt{13^2}$	97.2
Measurement repeatability of the chromatic confocal	97.2 nm	
(b) Combined uncertainty of the chromatic confocal	(b) $=\sqrt{(7)^2+(12)^2}$	313.7
© Combined uncertainty of the chromatic confocal interferometry		559.4
(4) Uncertainty of silicon wafer flatness	66.5	66.5
⑤ Uncertainty related to the thermal expansion of silicon wafer	$5.7 \cdot 10^{-8} \cdot L_1$	0.041
© Combined uncertainty (k=1)		563.3

Table S1 | Uncertainty analysis of the IR chromatic confocal spectral interferometry for the 725.4 μm silicon wafer

Source of uncertainty errors	Value	Value (nm) for L_0 =232 mm L_1 =777.5 μm and n=3.514
① Systematic uncertainty of the interferometry	$\sqrt{(2)^2 + (3)^2 + (4)^2}$	513.3
② Uncertainty of DFT algorithm $(L_1 \cdot n)$	512.9 nm	
③ Uncertainty of OSA (0.01 nm)	$6.6\times 10^{-6}\cdot L_1\cdot n$	
4 Uncertainty related to refractive index of air	$3.0\times 10^{-8}\cdot L_0$	
(5) Statistical uncertainty analysis of the interferometry	$\sqrt{6}^2$	52.5
Measurement repeatability of the interferometry	52.5 nm	
a Combined uncertainty of the interferometry	(a) $=\sqrt{(1)^2+(5)^2}$	516.0
Systematic uncertainty of the chromatic confocal	$\sqrt{8^2 + 9^2 + 10^2 + 11^2}$	298.3
(8) Uncertainty of LUT (OSA: 0.04nm/step)	296 nm	
Uncertainty of motor stage movement	$2.0\cdot 10^{-5}\cdot \frac{L_1}{n}$	
(10) Uncertainty of calibration mirror flatness	36 nm	
① Uncertainty of refractive index of air	$3.0\times 10^{-8}\cdot L_0$	
② Statistical uncertainty analysis of the chromatic confocal	$\sqrt{13^2}$	99.5
Measurement repeatability of the chromatic confocal	99.5 nm	
(b) Combined uncertainty of the chromatic confocal	(b) $=\sqrt{(7)^2+(12)^2}$	314.5
© Combined uncertainty of the chromatic confocal interferometry		561.5
(4) Uncertainty of silicon wafer flatness	66.5	66.5
⑤ Uncertainty related to the thermal expansion of silicon wafer	$5.7 \cdot 10^{-8} \cdot L_1$	0.044
© Combined uncertainty (k=1)		565.4

Table S2 | Uncertainty analysis of the IR chromatic confocal spectral interferometry for the 777.5 μm silicon wafer

Source of uncertainty errors	Thickness uncertainty value (nm)	Refractive value	Refractive index (n) for L_0 =232 mm L_1 =534.2 μm and n=3.514
① Combined uncertainty of the interferometry	356.8 (From Table 1)	-	-
② Combined uncertainty of the chromatic confocal	313.3 (From Table 1)	-	-
Combined refractive index uncertainty of the chromatic confocal interferometry	-	(a) = $\sqrt{\left(\frac{\partial n}{\partial_{int}}\right)^2 + \left(\frac{\partial n}{\partial_{conf}}\right)^2}$	0.00366
③ Uncertainty of silicon wafer flatness	66.5 (From Table 1)	-	-
4 Uncertainty by interferometry	233.7	-	-
⑤ Uncertainty by confocal	18.8	-	-
(b) Combined refractive index uncertainty of silicon wafer flatness	-	$(b) = \sqrt{\left(\frac{\partial n}{\partial_{int}}(4)\right)^2 + \left(\frac{\partial n}{\partial_{conf}}(5)\right)^2}$	0.00031
6 Uncertainty related to the thermal expansion of silicon wafer	0.03 (From Table 1)	-	-
① Uncertainty by interferometry	0.1	-	-
® Uncertainty by confocal	0.009	-	-
© Combined refractive index uncertainty related to the thermal expansion of silicon wafer	-	$(\widehat{C}) = \sqrt{\left(\frac{\partial n}{\partial_{int}}(\widehat{T})\right)^2 + \left(\frac{\partial n}{\partial_{conf}}(\widehat{S})\right)^2}$	0.0000001
© Combined uncertainty (k=1)	-		0.00367

Table S3 | Uncertainty analysis of refractive index measurement in IR chromatic confocal spectral interferometry for the 534.2 μm silicon wafer

	Chromatic confocal spectral interferometry [This research]	IR spectral interferometry ^{S1, S2, S3} [This research]	Industrial X-Ray computed tomography ^{S4, S5, S6}
Lateral resolution	14 μm	5 μm - few mm	1 - 100 μm
Repeatability (Vertical resolution)	72 nm - 102 nm	10 nm - 100 nm	~ 1 μm
Uncertainty (Precision)	150 nm - 340 nm	tens of nm ('N' Calibrated) – tens of μm ('N' uncalibrated)	1 - 100 μm
Acquisition time	0.8 second	0.01 - 1 second	1 second - 1 hour

Table S4 | Performance comparison of chromatic confocal spectral interferometry and alternative techniques

References

- S1. Jin, J., Kim, J. W., Kang, C.-S., Kim, J.-A. & Eom, T. B. Thickness and refractive index measurement of a silicon wafer based on an optical comb. *Opt. Express* **18**, 18339–18344 (2010).
- S2. Teh, W. H., Marx, D., Grant, D. & Dudley, R. Backside infrared interferometric patterned wafer thickness sensing for through-silicon-via (TSV) etch metrology. *IEEE Trans. Semicond. Manuf.* **23**, 419–426 (2010).
- S3. Schmitz, T. L., Davies, A., Evans, C. J. & Parks, R. E. Silicon wafer thickness variation measurements using the National Institute of Standards and Technology infrared interferometer. *Opt. Eng.* **42**, 2281–2290 (2003).
- S4. Gambino, J. P., Bowe, W., Bronson, D. M. & Adderly, S. A. Imaging of through-silicon vias using X-ray computed tomography. *Proc. 21st Int. Symp. Phys. Fail. Anal. Integr. Circuits* (IPFA), 327–330 (2014).
- S5. Sekhar, V. N. *et al.* Non-destructive testing of a high dense small dimension through silicon via (TSV) array structures by using 3D X-ray computed tomography method (CT scan). *Proc. 12th Electron. Packag. Technol. Conf. (EPTC)*, 462–466 (2010).
- S6. du Plessis, A., le Roux, S. G. & Guelpa, A. Comparison of medical and industrial X-ray computed tomography for non-destructive testing. *Case Stud. Nondestruct. Test. Eval.* **6**, 17–25 (2016).